Original scientific papers UDK 66.095.262−911.6
doi: 10.7251/COMEN1202131U

DEVELOPMENT OF A PORTABLE HUMAN SKIN DETECTOR BASED ON ACTIVE INFRARED ILLUMINATION

K. Uto[1,], H. Seki[1], T. Murase[2], S. Takagishi[2], Y. Kosugi[1]*

[1]Tokyo Institute of Technology, Interdisciplinary Graduate School of Science and Engineering, 4259 Nagatsuta, Midori-ku, Yokohama, 226-8502, Japan
[2] Sumitomo Electric Industries, LTD, 1-1-3, Konohana-ku, Osaka, 554-0024, Japan

Summary: A portable human skin detector based on a human skin index, NDHI, is introduced in this paper. The aim of system is at the safe, real-time and robust detection of human skin under various illumination conditions by the combination of the active pulse illumination of two low power LEDs, i.e. 1070 and 1550nm, with high frequency and the phase sensitive detection. The detection performance of the proposed system is evaluated under clear sky and in dark place.

Keywords: Human skin detection, infrared, active illumination, NDHI.

1. INTRODUCTION

Immediately after large-scale disaster, e.g. an earthquake, tsunami, storm, quick lifesaving is one of the top prioritized activities to mitigate the impact of disasters because of abrupt decrease in survival rate after 72 hours from the outbreak of the disaster. Automatic human detection based on remote sensing is an indispensable technology for immediate searching for casualties from a wide area. However, human body detection in remote sensing image is a big challenge. Human detection by range imager is feasible in case that the object is at close-range and the surrounding background is flat. However, the object detection at long-range from complicated backgrounds, e.g. debris, is difficult. Although thermal infrared imager is used for human detection from a wide area, it is difficult to detect human bodies with low biological activities. Motion-based detection based on optical sequential video images is not applicable when the victim is in low biological activities, or surrounded by other moving objects. Shape-based human detection is widely used in the computer vision filed. However, the detection is not feasible when only parts of human body are observable.

Human skin detection by means of spectral information is a promising methodology which overcomes the above-mentioned difficulties because the detection is possible without processing the spatial structure of objects. Human is the only object whose bare skin is exposed to air, so that the extraction of human skins from other various non-skin objects in background by characterizing the spectral difference between human skin and other objects is possible.

We have shown that a normalized difference human detection (NDHI) [1] based on two bands in shortwave infrared range, i.e. 1070 and 1550nm, performed satisfactory precision for human skin detection from various backgrounds.

For the actual situation of all-weather outdoor search of human body, a portable human skin detector capable of robust detection under various illumination conditions is required. The aim of this paper is a development of portable human skin detector based on active infrared illumination by which accurate detection under clear sky and in dark place is possible. At first, optical properties of human skin are briefly reviewed. Then, human indices defined by two bands in infrared range are introduced. A real-time, portable human detector based on active infrared illumination is proposed. Finally, the detection performance under 80,000 lux and 0 lux background illumination conditions is validated.

2. NORMALIZED DIFFERENCE HUMAN INDEX

2.1. Structure of human skin

Spectral characteristics of human skin have been widely investigated in the fields of cosmetics, computer vision and medicine. Since human is almost the only object whose bare skin is exposed to air, the structure contains protective function from

* Corresponding author: uto@pms.titech.ac.jp

sun exposure and bacteria, heat, cold and contact. The characterization of spectral feature in human skin is worthwhile for human detection.

Skin is composed of three layers, i.e. epidermis, dermis and subcutaneous tissue [2]. The epidermis, a 100μm-thick thin outer layer, is mainly composed of keratinocytes and melanocytes. The keratinocytes build a barrier against environmental damage. The melanin produced by the melanocytes acts as scattering media and pigments. The melanin has a protective role against harmful UV radiation. The lipid in the layer shows a pigment property.

The dermis is located between the epidermis and subcutaneous tissues. Thickness of the dermis varies from 1mm to 4mm. The dermis consists of connective tissue and contains blood vessels, lymph vessels, nerves, collagen, elastin, etc. The layer functions as protection from physical stress and regulation of temperature. The scattering property is mainly dependent on collagen and elastin fibers. Oxyhemoglobin and deoxyhemoglobin in the blood vessels, and water mainly define absorption properties of the dermis.

The third layer, the subcutaneous tissues, is 1-6mm thick. The layer contains fibrous bands, fat, blood vessels, etc. The scattering properties are affected by the connected tissues [3]. Lipid, hemoglobin and water are the principal pigments in subcutaneous tissues.

2.2. Human skin optical properties

The optical properties of human skin is well-approximated by various multi-layer reflection models composed of pigments and scattering properties, e.g. Kubelka-Munk theory based model [4], and Monte-Carlo based model [5]. Kubelka-Munk theory-based model is a simple model in which pigment absorption and two fluxes, i.e. forward and backward direction, are assumed. Monte-Carlo based model is a more rigorous stochastic model based on Monte Carlo techniques. In this section, we present a brief review of the optical properties of human skin.

The scattering in skin is caused by the interaction between particles in skin and photons. Small melanin dust, collagen and elastin fibrils (<30nm) causes Rayleigh scattering [6]. Large melanin particles (>300nm in diameter), lipids and proteins embedded in skin cause Mie scattering [6]. Results of experimental measurements of epidermis and dermis show a steady decrease of scattering coefficients with the increasing wavelength in visible-infrared range [3, 7]. The results are caused by (i) a decrease of contribution of Rayleigh scattering, and (ii) an increase of contribution of Mie scattering with increase of the wavelength.

The absorption coefficient of the melanin is peaked at ultraviolet range, and shows monotonic and smooth decline with an increase of the wavelength. The volume fraction of the epidermis occupied by melanosomes varies from 1.6% to 43% [8]. Oxyhemoglobin has absorption peaks at 415, 540 and 576nm which forms an m-shape absorption feature [9]. Deoxyhemoglobin has the absorption peaks at 430, 555, and 760nm [10]. There are a few narrow absorption peaks of water, i.e. strong absorption around 1430 and 1950nm, and weak absorption around 970 and 1200nm [11, 12]. The absorption peaks of lipid are 1710 and 1780nm [13]. In [14], the wavelength dependence of the absorption coefficient of human skin *in vitro* is observed. In visible range, the coefficient peaks are at 410, 540 and 575nm which are affected by the absorption of oxyhemoglobin. In infrared range, strong peaks are distributed around the absorption peaks of water and lipid, i.e. 1430, 1710 and 1780nm.

The optical penetration depth is dependent on the scattering property and the absorption property in skin. It is shown that the penetration depth varies with wavelength [14]. The depth is maximal at the range of 800-900nm and 1000-1100nm with the depth of up to 6-6.5mm. The findings indicate that reflectance of skin at the range of 800-900nm and 1000-1100nm is high because (1) the penetration depth is long enough to reach the subcutaneous tissue, and (2) the reflectance of the subcutaneous tissue at 800-900nm and 1000-1100nm is high [9]. On the other hand, that reflectance of skin at the range of 1400-1600nm is considerably low in comparison with the reflectance at 800-900nm and 1000-1100nm, because (1) the penetration depth is short due to the absorption of water and lipid, and (2) the reflectance of subcutaneous tissue at 1400-1600nm is low [9].

Figure 1 shows spectral profiles of human skin of mongoloid and other objects. The above-mentioned properties, e.g. m-shape oxyhemoglobin absorption at 540 and 576nm, high reflectance at 800-900nm and 1000-1100nm, low reflectance at 1400-1600nm, are confirmed. Since the spectral fluctuation by the variation of melanin contents in infrared range is considerably lower than that in a visible range [9], the characterization of human skin in infrared range containing 1000-1100nm and 1400-1600nm is expected to be robust. A range of 1350-1500nm, is removed to eliminate the strong vapor absorption range.

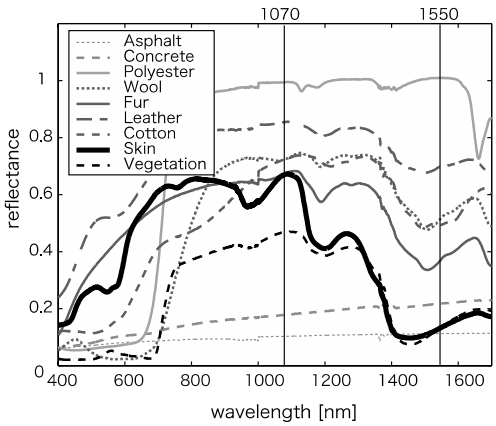

Figure 1. Spectral profiles of human skin and other objects.

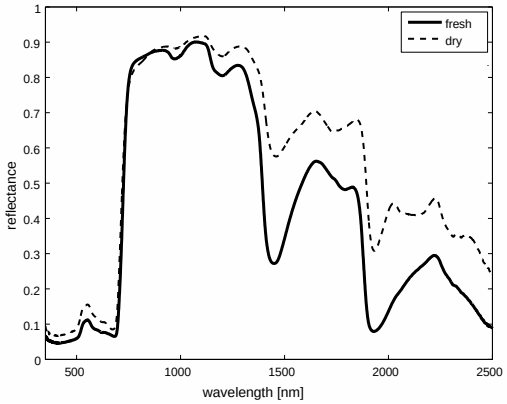

Figure 2. Reflectance of a fresh and dry oak leaf.

2.3. Normalized Difference Human Index

There are abundant applications of normalized difference indices in hyperspectral and multispectral remote sensing field [15-17]. Normalized difference indices are defined by a ratio of the difference between reflectances of two bands to the sum. Equation (1) is a definition of the normalized difference index.

$$NDI = \frac{\rho(\lambda_1)-\rho(\lambda_2)}{\rho(\lambda_1)+\rho(\lambda_2)} \quad (1)$$

where $\rho(\lambda_1)$ and $\rho(\lambda_2)$ are reflectances of wavelength λ_1 and λ_2. A normalized difference vegetation index (NDVI) [17], based on red and near-infrared bands, indicates high value for vegetation area, because spectral profiles of vegetation show steep increase in reflectance around 700nm, red edge, caused by chlorophyll absorption at red band and high reflectance at near-infrared (Figure 2). A normalized difference water index (NDWI) is introduced to detect water content of targets. The definition bands are near-infrared independent of water absorption, e.g. 860nm, and bands affected by water absorption, e.g. 1240, 1640, 2130 [15, 18, 19] (Figure 2). Spectral range in strong water absorption peaks, i.e. 1450n, and 1950nm, are eliminated in order to avoid the effect of water vapor.

Two almost identical normalized difference indices, i.e. NDHI [1] and NDSI [9], are proposed for human skin detection. The definition bands are pigment-free near-infrared range, 1000-1100nm, with high reflectance and range affected by water and lipid absorption with low reflectance, 1550-1600nm (Figure 1).

$$NDHI = \frac{\rho(1070)-\rho(1550)}{\rho(1070)+\rho(1550)} \quad (2)$$

$$NDSI = \frac{\rho(1080)-\rho(1580)}{\rho(1080)+\rho(1580)} \quad (3)$$

The distribution of NDHI values of human skin and other objects are shown in Figure 3. The NDHI values are calculated based on hyperspectral reflectance data collected by ASD FieldSpec® 3. The numbers of skin and other objects are 30 and 1400, respectively. It is confirmed that the NDHI values of human skin is above 0.6, whereas the NDHI values of other objects are distributed in the range below 0.6. Human skin extraction from various backgrounds based on NDHI is shown in Figure 4. The white regions in Figure 4(b) corresponds to NDHI>0.6. The pseudo-color image and the NDHI image are generated from a hyperspectral image acquired by a hyperspectral array sensor, 1000-1700nm range and 5nm spectral resolution.

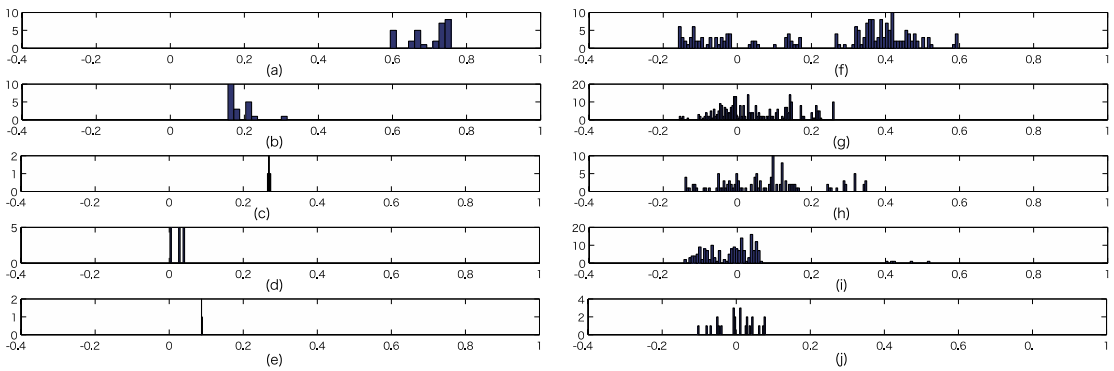

Figure 3. Distributions of NDHI values, (a) human skin, (b) cotton, (c) wool and fur, (d) polyester, (e) nylon, (f) vegetation, (g) steel, (h) asphalt and concrete,(i) plastic, and (j) glass.

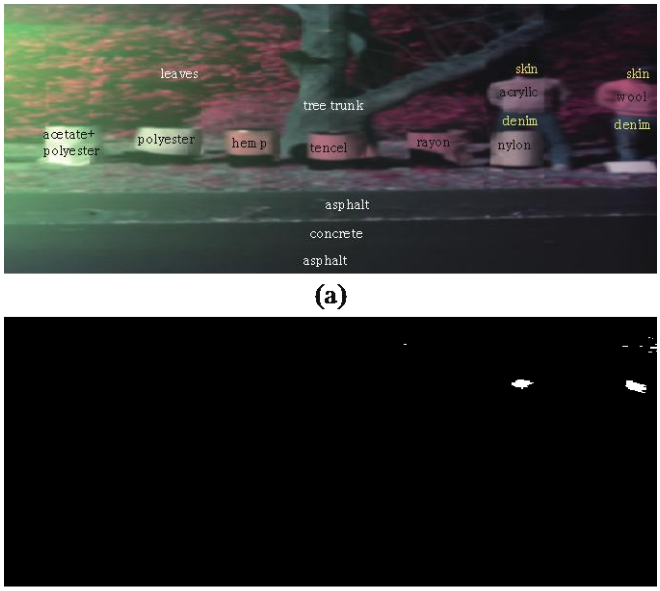

Figure 4. (a) Pseudo-color image (R,G,B) = (1144, 1477, 1585nm), (b) NDHI>0.6.

3. HUMAN SKIN DETECTOR BASED ON ACTIVE ILLUMINATION

3.1. Overview

NDHI is a reflectance-base index. Since reflectance is a ratio of the reflected flux to the incident flux, the acquisition of the spectral characteristics in illuminating light is required for detecting human skin under various conditions in illumination, e.g. cloudless sky, overcast and artificial light. For human search at night and in the dark places, the observation of reflected light is not feasible.

Active narrow-band infrared LED illumination sensing system is a promising tool which overcomes the above-mentioned difficulties because the spectral profile of incident illumination is known and the acquisition of reflected light under low background light is possible. In this section, a human skin detector based on active infrared illumination is introduced (Figure 5).

The reflection flux based on active illumination corresponds to the difference between reflection flux under active illumination and the flux under non-illuminated condition. The reflectance is calculated based on the observed reflection flux and the specification of illumination. Reflection of two NDHI-related bands is collected by generating a pair of mutually exclusive pulse train signals corresponding to two bands.

The illumination is generated from low power LEDs to protect eye and skin from damage. In order to extract reliable information from the noisy signals due to the low level illumination, the observed signals are processed by the phase-sensitive detector (PSD). NDHI is derived based on the PSD outputs correspond to the NDHI-related bands.

The processing flow is shown in figure 6.

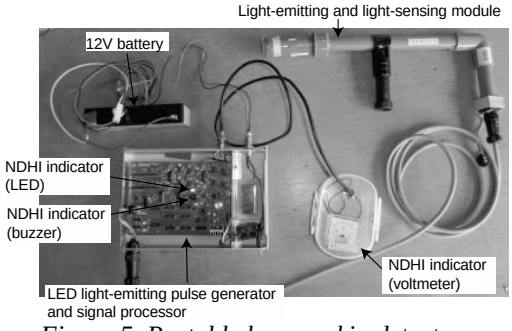

Figure 5. Portable human skin detector.

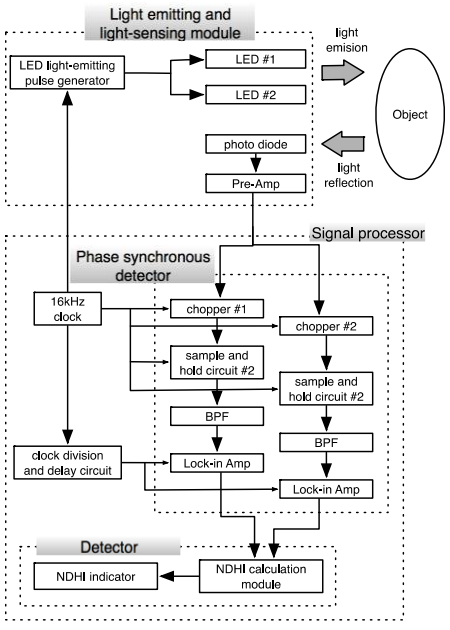

Figure 6. Flow of process.

3.2. Light emitting and light sensing module

Two NDHI-related low power LED modules, LED #1 and #2, are driven by light pulse train patterns generated by a LED light-emitting pulse generator. The light pulse train patterns are shown in Figure 7(a). The pulse width is determined by the frequency of the clock, e.g. 62.5μs for 16kHz clock.

The reflected light is sensed by an InGaAs photodiode with a spectral response range from 1000 to 1700nm. The time constant, e.g. 66nm, is considerably shorter than the pulse width, so that the sensor output shows prompt response to the input pulse trains. The input at the lighting phase is a sum of the LED illumination and background light, and the input at the non-lighting phase is the background light. The sensor response is a sum of the response to the input illumination and noise. The sensed data are amplified in a pre-amplifier, then sent to a signal processor.

The light-emitting and light-sensing module is shown in Figure 8. The maximum permissible exposures (MPE) defined in IEC 60825-1[20] and power of the emitted lights are shown in Table 1 in which sufficient safety of the system is guaranteed.

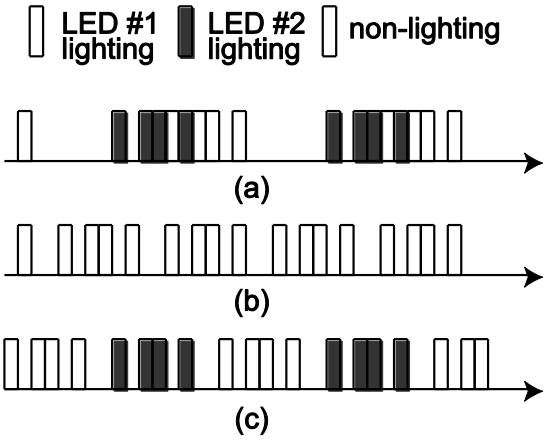

Figure 7. (a) LED light-emitting pulse trains, (b) chopping signal #1, (c) chopping signal #2.

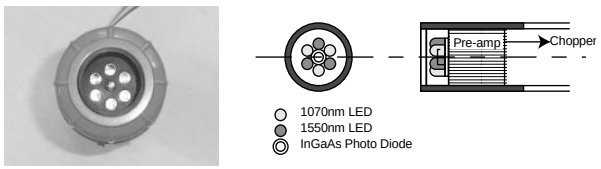

Figure 8. Light-emitting and light-sensing module.

Table 1. The maximum permissible exposures and power of the emitted lights.

	1070nm	1550nm
MPE (human skin)	1 W/cm^2	100 mW/cm^2
MPE (human cornea)	1.78 mW/cm^2	100 mW/cm^2
NDHI sensor	0.22 mW/cm^2	0.27 mW/cm^2

3.3. Signal processor

The signal processor is a combination of a phase synchronous detector and a detector module. The phase synchronous detector is composed of a pair of choppers, sample-and-hold circuits, bandpass filters and lock-in amplifiers [21]. The choppers, sample-and-hold circuits and lock-in amplifiers are operated based on clock signals.

The output of the amplified sensor is sampled by the chopper circuits based on chopping signals in Figure 7(b) and (c). The sampling signals in Figure 7(b) and (c) are periodic patterns that consist of a lighting period and a non-lighting period. The sampled signals by the chopper #1 and #2 are sent to the sample-and-hold circuits. In the sample-and-hold circuits, the sampled signal levels are hold at a constant level while the lighting intensities are constant. Figure 9 shows simulation results. In Figure 9(a), the high and low level pulses correspond to sampled signals under the lighting period and non-lighting period, respectively. The output of the sample-and-hold circuit is shown in Figure 9(b). The high frequency components are removed by CR low-pass filter. The output patterns by the sample-and-hold circuit #1 and #2 are signals with the identical frequency and phase shift $\pi/2$.

The rectangular output waves from the sample-and-hold circuits are sent to narrow bandpass filters whose target period is 16 times the pulse width. The output signals are sinusoid waves as shown in Figure 9(c).

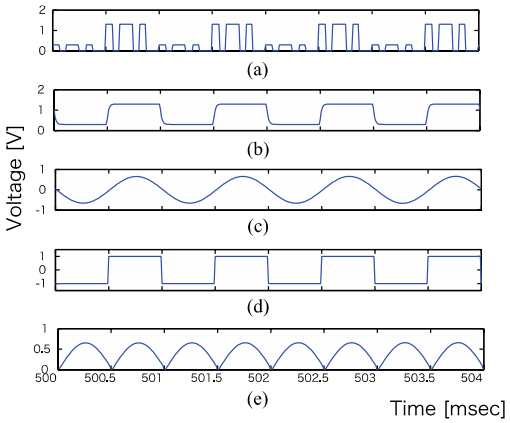

Figure 9. Simulation results, (a) sampled signal, (b) output of sample-and-hold circuit, (c) output of bandpass filter, (d) detection reference, and (e) phase sensitive detection output.

In the lock-in amplifiers, the reflection response corresponding to the active illumination is extracted by the phase synchronous detection based on detection reference signal shown in Figure 9(d). The reference signals are generated in the clock division and delay circuit in which the clock signal is

divided by 16. The phase shift between the two reference signals is $\pi/2$. The output of the lock-in amplifier is shown Figure 9(e). The peak level of the output is proportional to the reflection intensity by the active LED illumination. The detected signals are converted to DC signals by low-pass filters or sample-and-hold circuits. The DC signals related to the reflection intensities based on the LED #1 and #2, V_1 and V_2, are sent to the human skin detection module.

3.4. Human skin detection module

The human skin detection module is composed of a NDHI calculation module and a NDHI indicator. In the NDHI calculation module, the addition and subtraction results, i.e. V_1+V_2 and V_1-V_2, are sent by operational amplifiers to an analog divider. The output voltage of the divider is linearly correlated to NDHI.

In order to derive reflectance-based NDHI, a standard white diffuse reference is observed, then variable resistance of the circuit are adjusted so as to make the addition voltage larger, while the subtraction is zero. The updating period of the NDHI value is 1msec on condition of 16kHz clock, so that real-time detection is possible.

The NDHI indicator is composed of a voltmeter, a buzzer and a LED light. In case the NDHI exceeds the given threshold, e.g. 0.7, human skin detection is notified by lighting and sound.

4. EXPERIMENT

Close-range objects at a distance of 40 centimeters from the sensor are observed under background illumination conditions of clear sky (80,000 lux) and a dark room (0 lux). The targets are human skins, sausage, chicken skin, chicken meat, chicken leaves, wood, soil, cotton, fabrics, and polyester fabrics. The NDHI-related voltage and NDHI values based on hyperspectral data acquired by ASD FieldSpec® 3 are shown in Table 2 and Figure 10. The values of human skins are mean of palms and backs of hands of three subjects (Mongoloid). The values of other materials are means of five observations. Sausage is selected as a high NDHI object because it is shown that small intestine epitheliums of the mammals indicate high NDHI values [22].

The markers in the fifth column in Table 2 correspond to the markers in Figure 10. The correlation between the NDHI-related voltages and the NDHI values is high, i.e. R^2=0.97. The detection performance of damaged bodies based on the proposed system is validated by the high NDHI value of human skin, chicken skin and meat (>0.41). The NDHI-related voltages under 80,000 lux are highly correlated with the voltages under 0 lux, i.e. R^2=0.9991. The accurate detection under various background light conditions is feasible using the proposed system.

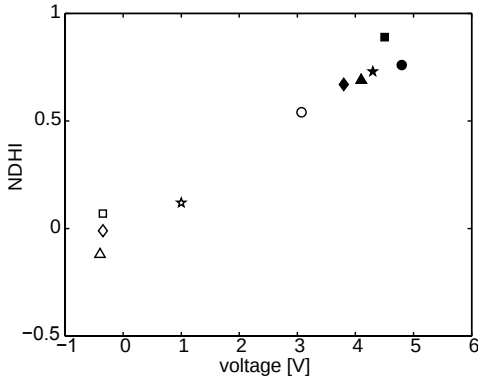

Figure 10. Relation between NDHI-related voltages and NDHIs.

Table 2. NDHI-related voltages and NDHIs

Object	NHDI	Voltage		Marker
		daylight	Dark room	
Human skin	0.76	4.8	4.8	●
Sausage	0.73	4.3	4.4	★
Chicken (skin)	0.69	4.1	-	▲
Chicken (meat)	0.89	4.5	-	■
Chicken (bone)	0.67	3.8	-	♦
Leaf	0.54	3.1	3.0	○
Wood	0.12	1.0	0.90	☆
Soil	-0.12	-0.40	-0.40	△
Cotton	0.07	-0.35	-0.34	□
Polyester	-0.01	-0.35	-0.35	◇

5. CONCLUSION

After a brief review of optical properties of human skin, two characteristic bands, 1000-1100n, and 1400-1600nm, which differentiate human skin from other objects, are identified. Human skin index based on the bands is introduced. In order to realize the robust detection under various illumination conditions, a portable human detector based on active infrared illumination is proposed. It is confirmed that the proposed system accomplishes real-time, accurate and robust detection under clear sky and in dark place.

The ongoing development of long-range object detection system is aiming at search for missing human bodies in practical situations. The expansion of the targeting range is realized by the combination of (i) the parallel light beam generated by a parabolic reflector and a light source and (ii) the focusing viewing angle by a telephotographic lens in front of the sensor, e.g. the viewing diameter at 10 meter from the detector is 27mm.

6. REFERENCES

[1] T. Edanaga, K. Uto, and Y. Kosugi, *Studies on the extraction of human skin using spectral information in shortwave infrared band*, Journal of the Japan Society of Photogrammetry and Remote Sensing, Vol. 46 (2007) 17−26.

[2] R. R. Anderson and J. A. Parrish, *The Optics of Human Skin*, J Investig Dermatol, Vol. 77 (1981) 13−19.

[3] E. Salomatina, B. Jiang, J. Novak, and A. N. Yaroslavsky, *Optical properties of normal and cancerous human skin in the visible and near-infrared spectral range*, Journal of Biomedical Optics, Vol. 11 (2006) 064026-9.

[4] M. Doi and S. Tominaga, *Spectral estimation of human skin color using the Kubelka-Munk theory*, SPIEIST Electronic Imaging, Vol. 5008 (2003) 221−228.

[5] S. T. Flock, M. S. Patterson, B. C. Wilson, and D. R. Wyman, *Monte Carlo modeling of light propagation in highly scattering tissue--I: Model predictions and comparison with diffusion theory*, IEEE transactions on bio-medical engineering, Vol. 36 (1989) 1162−8.

[6] I. S. Saidi, S. L. Jacques, and F. K. Tittel, *Mie and Rayleigh modeling of visible-light scattering in neonatal skin*, Appl. Opt., Vol. 34 (1995) 7410−7418.

[7] A. N. Yaroslavsky, P. C. Schulze, I. V. Yaroslavsky, R. Schober, F. Ulrich, and H. J. Schwarzmaier, *Optical properties of selected native and coagulated human brain tissues in vitro in the visible and near infrared spectral range*, Physics in Medicine and Biology, Vol. 47 (2002) 2059-2073.

[8] S. L. Jacques, *Origins of tissue optical properties in the UVA, Visible, and NIR regions*, OSA TOPS on Advances in Optical Imaging and Photon Migration, Vol. 2 (1996) 364−370.

[9] A. S. Nunez, *A Physical Model of Human Skin and Its Application for Search and Rescue*, PhD, Graduate School of Engineering and Management, AIR Force Institute of technology, Ohio 2009.

[10] G. Zonios, J. Bykowski, and N. Kollias, *Skin melanin, hemoglobin, and light scattering properties can be quantitatively assessed in vivo using diffuse reflectance spectroscopy*, The Journal of investigative dermatology, Vol. 117 (2001) 1452−1457.

[11] L. Kou, D. Labrie, and P. Chylek, *Refractive indices of water and ice in the 0.65- to 2.5-μm spectral range*, Applied Optics, Vol. 32 (1993) 3531-3540.

[12] D. M. Wieliczka, S. Weng, and M. R. Querry, *Wedge shaped cell for highly absorbent liquids: infrared optical constants of water*, Applied Optics, Vol. 28 (1989) 1714−1719.

[13] K. A. Martin, *Direct measurement of moisture in skin by NIR spectroscopy*, Journal of the Society of Cosmetic Chemists, Vol. 261 (1993) 249−261.

[14] A. Bashkatov, E. Genina, V. Kochubey, and V. Tuchin, *Optical properties of human skin, subcutaneous and mucous tissues in the wavelength range from 400 to 2000 nm*, *Journal of Physics D: Applied Physics*, Vol. 38 (2005) 2543−2555.

[15] B. C. Gao, *NDWI-A normalized difference water index for remote sensing of vegetation liquid water from space*, Remote Sensing of Environment, Vol. 58 (1996) 257−266.

[16] J. A. Gamon, J. Penuelas, and C. B. Field, *A narrow-waveband spectral index that tracks diurnal changes in photosynthetic efficiency*, Remote Sensing of Environment, Vol. 41 (1992) 35−44.

[17] J. W. Rouse, R. H. Haas, J. A. Schell, and D. W. Deering, *Monitoring vegetation systems in the Great Plains with ERTS*, Proceedings of the Third ERTS Symposium, 1973, 309−317.

[18] R. Fensholt and I. Sandholt, *Derivation of a shortwave infrared water stress index from MODIS near- and shortwave infrared data in a semiarid environment*, Remote Sensing of Environment, Vol. 87 (2003) 111−121.

[19] D. Chen, J. Huang, and T. J. Jackson, *Vegetation water content estimation for corn and soybeans using spectral indices derived from MODIS near- and short-wave infrared bands*, Remote Sensing of Environment, Vol. 98 (2005) 225−236.

[20] I. E. Commission, *Safety of laser products*, in Part 1: Equipment classification and requirements vol. IEC 60825-1, ed: International Electrotechnical Commission, 2007.

[21] P. A. Temple, *An introduction to phase-sensitive amplifiers: An inexpensive student instrument*, American Journal of Physics, Vol. 43 (1975) 801−801.

[22] H. Akbari and Y. Kosugi, *Hyperspectral Imaging: a New Modality in Surgery*, in Recent Advances in Biomedical Engineering, G. R. Naik, Ed., ed: InTech, 2009, 223−240.

ꕥ

РАЗВОЈ ПРЕНОСИВОГ ДЕТЕКТОРА ЉУДСКЕ КОЖЕ НА ОСНОВУ АКТИВНОГ ИНФРАЦРВЕНОГ ОСВЈЕТЉЕЊА

Сажетак: У овом раду је описан преносиви детектор људске коже заснован на индексу људске коже, NDHI. Циљ система је сигурно и робусно откривање људске коже у стварном времену у различитим условима осветљења, комбинацијом активног импулсног осветљења двије LED мале снаге, одн. од по 1070 и 1550 nm, мале фреквенције и фазно-осјетљиве детекције. Перформансе детекције предложеног система оцјењиване су у условима ведрог неба и на мрачном мјесту.

Кључне ријечи: детекција људске коже, инфрацрвено, активно осветљење, NDHI.

ꕥ